VERTEBRATE ZOOLOGY

68 (1): 65–82
19.4.2018
SENCKENBERG

Functional morphology of the lungs of the green iguana, *Iguana iguana*, in relation of body mass (Squamata: Reptilia)

Danilo Peixoto[1], Wilfried Klein[2,4], Augusto Shinya Abe[3,4] & André Luis da Cruz[1,4,*]

[1] Federal University of Bahia, Institute of Biology, Laboratory of Animal Physiology. Rua Barão de Geremoabo s/n, Ondina, CEP 40170-970 – Salvador, Bahia, Brazil — [2] School of Philosophy, Sciences and Literature of Ribeirão Preto, University of São Paulo (USP), Avenida Bandeirantes, 3900. Monte Alegre – CEP 14040-90, Ribeirão Preto, São Paulo, Brazil — [3] São Paulo State University, Rio Claro Campus, Institute of Biosciences, Avenida 24-A, 1515. Bela Vista – CEP 13506-900 – Rio Claro, São Paulo, Brazil — [4] National Institute of Science and Technology in Comparative Physiology, Rio Claro, São Paulo, Brazil — * Corresponding author; Tel.: +55 (71) 32836560; cruz.andre@ufba.br

Accepted 4.ix.2017.
Published online at www.senckenberg.de/vertebrate-zoology on 5.4.2018.

Editor in charge: Axel Zarske

Abstract

Body mass is one of the most influencing factors of metabolic rate and gas exchange of animals, and also related to activity pattern and occupancy of ecological niches. This study aimed to understand the relationships between body mass (M_B) and morpho-functional features of the lungs of *Iguana iguana,* through morphological and morphometric characterization of the structural elements of the respiratory system. *Iguana iguana* has lungs of the transitional type, the heterogeneously distributed parenchyma being faveolar in cranial and medial regions and trabecular in the caudal region. Within the parenchyma, 43.6±25.5% corresponds to faveoli, 18.0±5.9% to interfaveolar septa, and 38.7±31.6% to trabeculae. Within the interfaveolar septa, 9.4±4.0% corresponds to blood capillaries, 4.4±1.0% to type I pneumocytes and 3.9±1.1% to type II pneumocytes. Allometric analyses showed that lung ($M_B^{0.8949}$) and parenchymal volume ($M_B^{1.030}$) scale with M_B in *I. iguana* just as in other lizards with unicameral or transitional lungs, which was unexpected for lung volume, since reptilian lung volume is generally considered to scale as $M_B^{0.75}$. The functional morphology of the lungs in *I. iguana* seems to play an important role to meet the metabolic demands through ontogenetic growth.

Key words

Lizard, respiratory morpho-functionality, gas exchange.

Introduction

In terms of pulmonary morphology, reptiles form an interesting intermediate state between birds and mammals (Powell & Hopins, 2004), since these ectotherms exhibit extremely diverse lung morphologies, showing variations in structural lung type and distribution as well as kind of parenchyma (Wolf, 1933; Meban, 1978; Klaver, 1979; Klemm *et al*., 1979; Luchtel & Kardong, 1981; Stinner, 1982; Perry, 1983, 1988, 1998; Perry *et al*., 1989). Among squamates, significant variations regarding the structural pulmonary type and distribution and kind of lung parenchyma are also well known (Perry, 1998). A recently proposed scenario for the evolution of the amniote respiratory system suggests that the last common ancestor of amniotes possessed multi-chambered lungs that evolved into single-chambered lungs among the Lepidosauria due to the small body size of stem

lepidosauromorphs (Lambertz *et al.*, 2015). The multichambered lungs found in the Gila monster *Heloderma suspectum* and monitor lizards of the genus *Varanus* are being interpreted as having secondarily evolved in this lineage from a simpler lung structure, since a multichambered stage can be identified during the ontogeny of a gekkotan single-chambered lung (Lambertz *et al*., 2015). Superimposed onto these evolutionary traits are the various metabolic demands that the respiratory system has to serve (Powell & Hopkins, 2004). Typically, reptiles show low metabolic rates compared to endothermic vertebrates with similar body mass (Powell & Hopkins, 2004), but the great diversity of lifestyles and habits resulted in a large variation in metabolic demands and distinct morpho-functional respiratory adaptations. To maintain increased metabolic rates, a larger respiratory surface area is required, achieved through increased pulmonary compartmentalization. Monitor lizards, for example, show elevated metabolic demands due to their pattern of activity and larger body mass and have lungs more compartmentalized than less active species and with lower body mass (Maina *et al*. 1989).

The effects of body mass on reptilian metabolism have been widely studied (e.g. Van Marken-Lichtenbelt *et al*. 1993, Dawson & Bartholomew 1956, Wood et al. 1978, Andrews & Pough 1985, McNab 2002, Maxwell *et al*. 2003) and it has been verified that intraspecifically an increase in body mass results in an increase in the total metabolic rate and in the density of respiratory surfaces. However, among lizards, Bennett & Dawson (1976), Beuchat & Vleck (1990), Karasov & Anderson (1998) reported no significant metabolic changes between hatchling and adult iguanids. So, if intraspecific metabolic changes do not occur along with variations in body mass, it is expected that, proportionately, the density of respiratory surfaces is kept mass independent. In order to verify this relationship we choose the species *Iguana iguana* as experimental model, belonging to the family Iguanidae. This species shows a more than 350 fold increase in body mass from hatchling to adult (12 g – 4.5 kg), allowing to study pulmonary morphology in animals of various body sizes. Thus, this study aimed to investigate the relationships between morpho-functional aspects of the lungs in *Iguana iguana* of different body masses through morphological and morphometric characterization of the structural elements of the respiratory system, which potentially are determinant for metabolic rate and thereby activity of the species.

Material and methods

Animals

Five iguanas of different body masses (M_B; 0.020, 0.026, 0.319, 0.546, and 2.4 kg) were obtained from the same population of animals being held and reproduced at the Jacarezário, São Paulo State University "Julio de Mesquita Filho" Rio Claro, SP, Brazil, the two smaller animals having hatched recently, the two intermediate animals being 1 year old and the largest animal being 2 years old. The animals were killed by an overdose of Sodium Thiopental (100 $mg.kg^{-1}$), administered intraperitoneally (018/2014 Protocol of the Committee on Animal Use and Ethics, IBIO/UFBA). Subsequently, the lungs were fixed by means of intratracheal instillation of glutaraldehyde 5% in 0.2 M phosphate buffer (pH 7.4, 380 mOsm) at a pressure of 20 cmH_2O for 12 hours. Following fixation the lungs were removed, stored for up to 10 days in glutaraldehyde 0.5% stock solution in 0.2 M phosphate buffer (pH 7.4; 380 mOsm) for light and electron microscopical processing.

Respiratory system measurements

The following variables regarding the respiratory system have been measured (adopted from Klein *et al*. (2005): length of the left lung (L_{le} [mm]) and length of the right lung (L_{ri} [mm]). To remove the effect of body size, the ratio of L_{le}/L_{ri} was calculated.

Total volume pulmonary determination

The total lung volume was determined by the Cavalieri method that estimates the total volume and area of cross sections multiplied by the distance between the sections (Cruz-Orive & Weibel 1990). For this purpose, the size of each lung was measured in cranio-caudal direction and ten cross sections were performed from a random starting point and in fixed distances, based on the total length of each lung. A test system was superimposed on the cross sections and the numbers of points covering lung parenchymal and lung lumen were counted (Fig. 1A). The total volume (V_L) of the lungs was given by:

$$V = T.a/p.\Sigma Pi,$$

where "T" is the distance between sequential sections, "a/p" is the area represents by each point and "Pi" is the number of points over the parenchyma and lumen. To estimate the parenchymal and lumen volume separately, the same methodology was applied by counting the points over each structure.

Relative lung volume (V_L/M_B), relative parenchymal volume (V_P/V_L) and the ratio of parenchymal volume and body mass were obtained by multiplication of the first two parameters ($[V_P/V_L].[V_L/M_B]$).

Morphometric parameters and sampling

The cranial, medial and caudal regions of the lungs of each specimen were separated for analysis and using a stereoscopic microscope samples of 5 mm^2 of these areas were removed (N = 5) and used for the histological

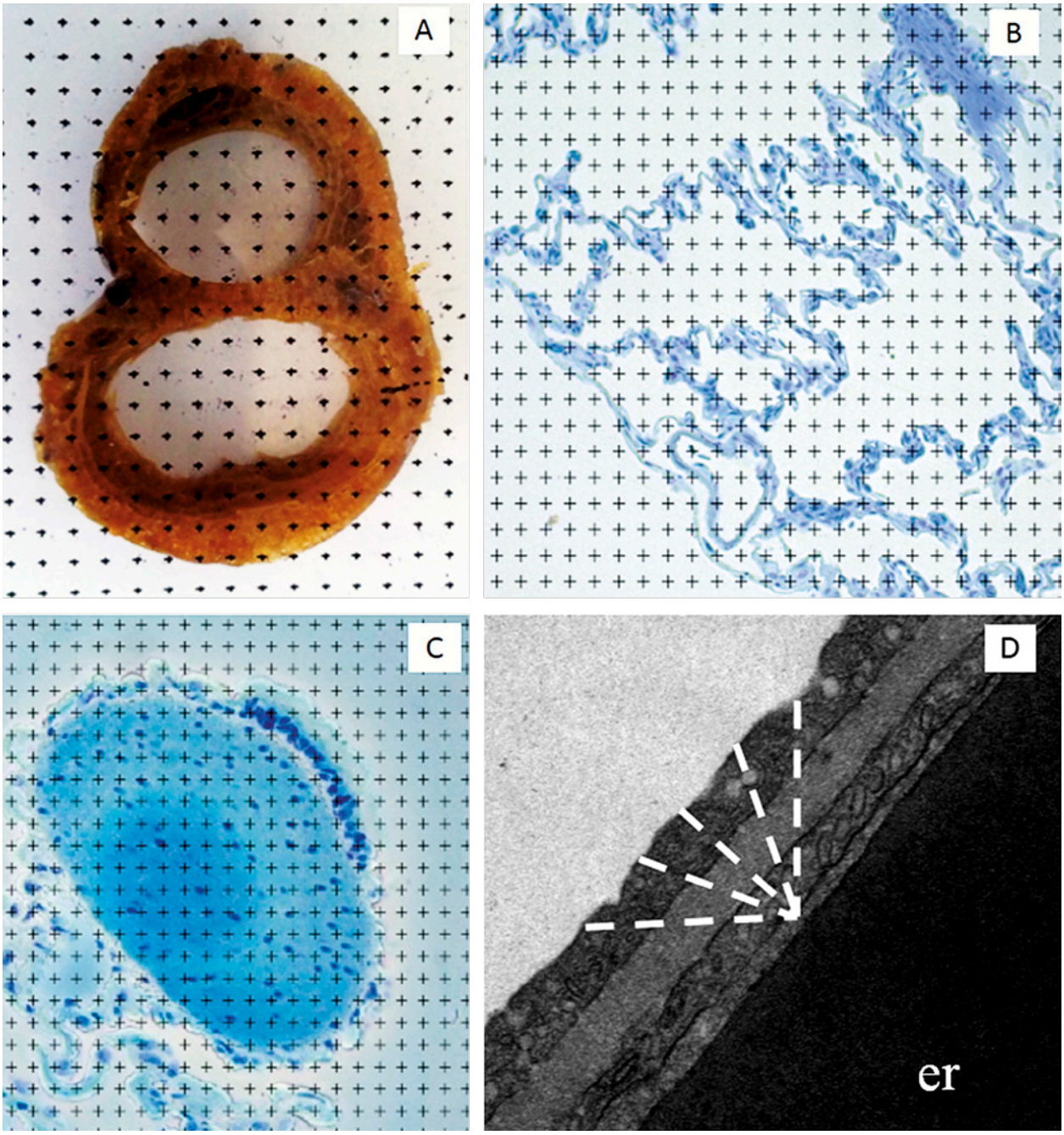

Fig. 1. (A) Cross section of *Iguana iguana* lungs with point test system used to quantify total lung volume, parenchymal volume and lumen volume. (B) Longitudinal section of the lung parenchyma of the *Iguana iguana* with test point system used to quantify the volume density (Vv) of the main components of the parenchyma. (C) Longitudinal section of trabeculae with test point system used to quantify the major components of trabeculae. (D) Measurement of the distance of the air-blood diffusion barrier representing the possible angles used to determine diffusion distance. Erythrocyte (er).

processing for light microscopy and transmission electron microscopy, whereas subsamples of 0.5 mm^2 (N = 5) were used for scanning electron microscopy.

Morphological analysis

Stereomicroscopy. Samples of the cranial, medial and caudal regions were analyzed and photomicrographed using a Leica M165C stereomicroscope coupled to digital camera DFC 450 and the images were used to characterize the internal pulmonary anatomy.

Light microscopy. The samples for light microscopy were dehydrated in a graded series of ethanol with their pleural surface facing down and were systematically rotated and sectioned in order to obtain vertical uniform sections (VUR), according to Howard & Reed (2005). Subsequently, they were embedded in methacrylate (Historesina® Leica).

Histological sections of 5 µm were cut using a manual Zeiss Hyrax M15 microtome, mounted on slides, stained with toluidine blue (1%) and photomicrographed using a Zeiss Axio Lab.A1 and capture software Vision Rel. 4.8. The images were used for structural characterization and quantitative analysis.

Transmission electron microscopy. The samples for transmission electron microscopy were post-fixed in osmium tetroxide 1%, 0.8% potassium ferrocyanide and 5 mM calcium chloride in 0.1 M sodium cacodylate buffer, pH 7.4 for one hour. They were washed three times for ten minutes each in the same buffer, dehydrated in a graded series of acetone, followed by three successive baths of 100% acetone and subsequent replacement of the acetone and Polybed® resin (1:1) for 6 hours. Afterwards the samples were transferred to pure resin, where they remained until polymerization.

Semithin (0.5 µm) and ultrathin (80 nm) sections were performed using an ultramicrotome Leica EM UC7. The ultrathin sections were stained using uranyl acetate and lead citrate, and analyzed with a transmission electron microscope JEOL 1230. The images were used for ultrastructural characterization and measurement of the distance of the air-blood diffusion barrier.

Scanning Electron Microscopy. The subsamples designated for scanning electron microscopy (SEM) were dehydrated through a crescent ethanol series and passed through drying by Critical Point in a Leica CPD 030. Subsequently, the samples were plated in gold and analyzed by scanning electron microscope JEOL JSM 6390LV.

Quantitative analysis

The quantitative analyzes were performed based on the method of Cruz-Orive & Weibel (1990) and Howard & Reed (2005).

Volume density (Vv). The volume densities of the parenchymal components (faveoli, septa, trabeculae, type I and type II pneumocytes) were estimated by the ratio between the points over the different components and the reference area (Fig. 1B). This way:

$$V_{vcp} = \Sigma P(cp)/\Sigma P(ref),$$

where, $\Sigma P(cp)$ gives the sum of the points over the component to be estimated (faveoli, septa, trabeculae, type I or type II pneumocyte, respectively) and $\Sigma P(ref)$ gives the sum of the points over the reference space (faveoli + septa + trabeculae + type I + type II pneumocytes). A total of 1.125 micrographs were quantified at a final magnification of 200×. The estimate of the volume density of the trabeculae was given by the ratio between the points on the component to be estimated (muscle or capillary) and the points on the volume of reference (muscle + capillary) (Fig. 1C). A total of 20 micrographs were quantified at a final magnification of 400×.

Thickness of air-blood barrier. To determine the thickness of the blood-air diffusion barrier between the surface of the epithelium and the endothelial cell surface, ten electron micrographs of cranial, medial and caudal regions from three specimens (0.020; 0.319; 2.4 kg) were used, totaling 30 micrographs for each specimen, at a final magnification of 25.000×. On each micrograph the distance of the air-blood diffusion barrier at an angle defined by random from among five different angles (0º, 45º, 90º, 135º, 180º) was measured (Fig. 1D). These were used to obtain the arithmetic mean and standard deviation. The measurements were performed using Image J® software.

Statistical analysis

The descriptive statistics (mean and standard deviation) and Pearson correlation coefficient and simple linear regression were calculated using the Biostat® 5.3 software. Linear regression analyses were performed using GraphPad Prism 6. A statistical difference was considered significant at $P < 0.05$.

Results

Pulmonary anatomy

Macroscopically lungs of all *Iguana iguana* were very similar, showing a pair of saccular lungs of different sizes, with the right lung being longer than the left one (L_{le}/L_{ri}: 0.84 ± 0.03) (Fig. 2A; Table 1), and with short extrapulmonary bronchi fused medially near the region of entrance into the lungs (Fig. 2B). Both lungs were situated in the pleuroperitoneal cavity, ventral to the digestive tract, laterally limited by dorsal ribs, intercostal muscles and the dorsal spine.

In cross section, the lungs were oval-shaped and composed of two chambers, separated by a longitudinal septum, characterizing it as a transitional lung (Fig. 2C). The smaller cranial chamber originated in the medial region and extended to the cranial region and the larger caudal chamber originated in the cranial region and extended through the medial to the caudal region. In longitudinal section two distinct epithelial types were present, the cranial and medial regions with pronounced faveoli and a relatively small lung lumen, and the caudal region com-

→ **Fig. 2.** (A) Ventral view of *Iguana iguana* (M_B=2.4 kg) lungs. (B) Dorsal view of the lungs showing the medial fusion of the bronchi (arrow). (C) Cross-section of a lung. (D) Lateral view of the medial half showing the transitional region of parenchyma (arrow). Cranial chamber (crc), caudal chamber (cac), trachea (tr), right lung (L_{ri}) and left lung (L_{le}), faveolar region (fvr), trabecular region (trr), hilus (hi).

Table 1. Body mass (M_B), length of the left lung (L_{le}), length of the right lung (L_{ri}), ratio of L_{le}/L_{ri}, total volume of the lungs (V_L), volume parenchyma (V_P), and lumen volume (V_{Lum}) of *Iguana iguana* lungs.

Animal	M_B (kg)	L_{le} (mm)	L_{ri} (mm)	L_{le}/L_{ri}	V_L (cm^3)	V_P (cm^3)	V_{Lum} (cm^3)
1	0.020	24.3	27.4	0.89	6.7	0.8	5.9
2	0.026	25.4	29.5	0.86	8.6	1.2	7.3
3	0.319	65.8	80.7	0.82	90.7	16.5	74.1
4	0.546	78.0	92.8	0.84	130.2	25.9	104.3
5	2.4	107.6	131.3	0.82	478	122	356

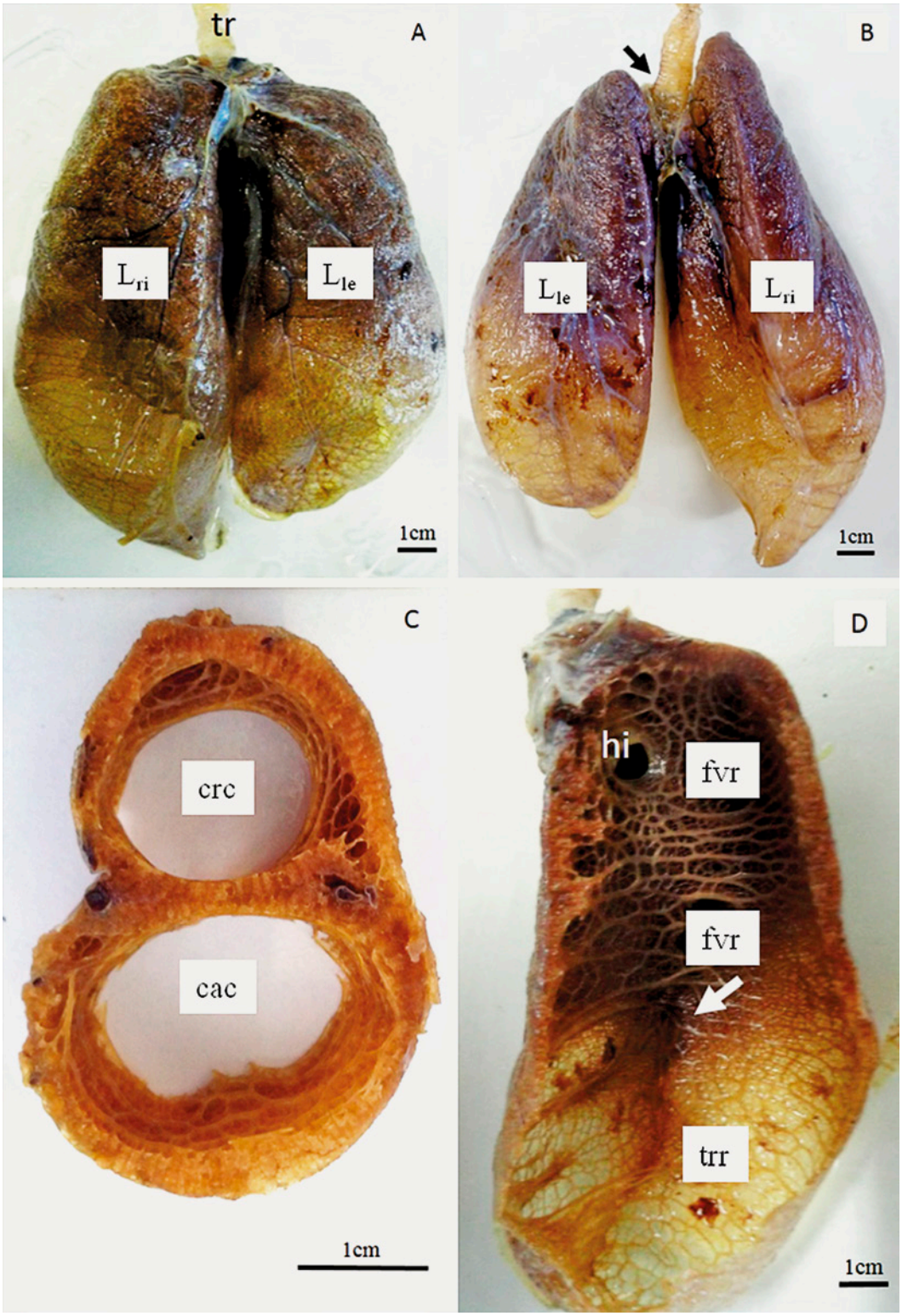

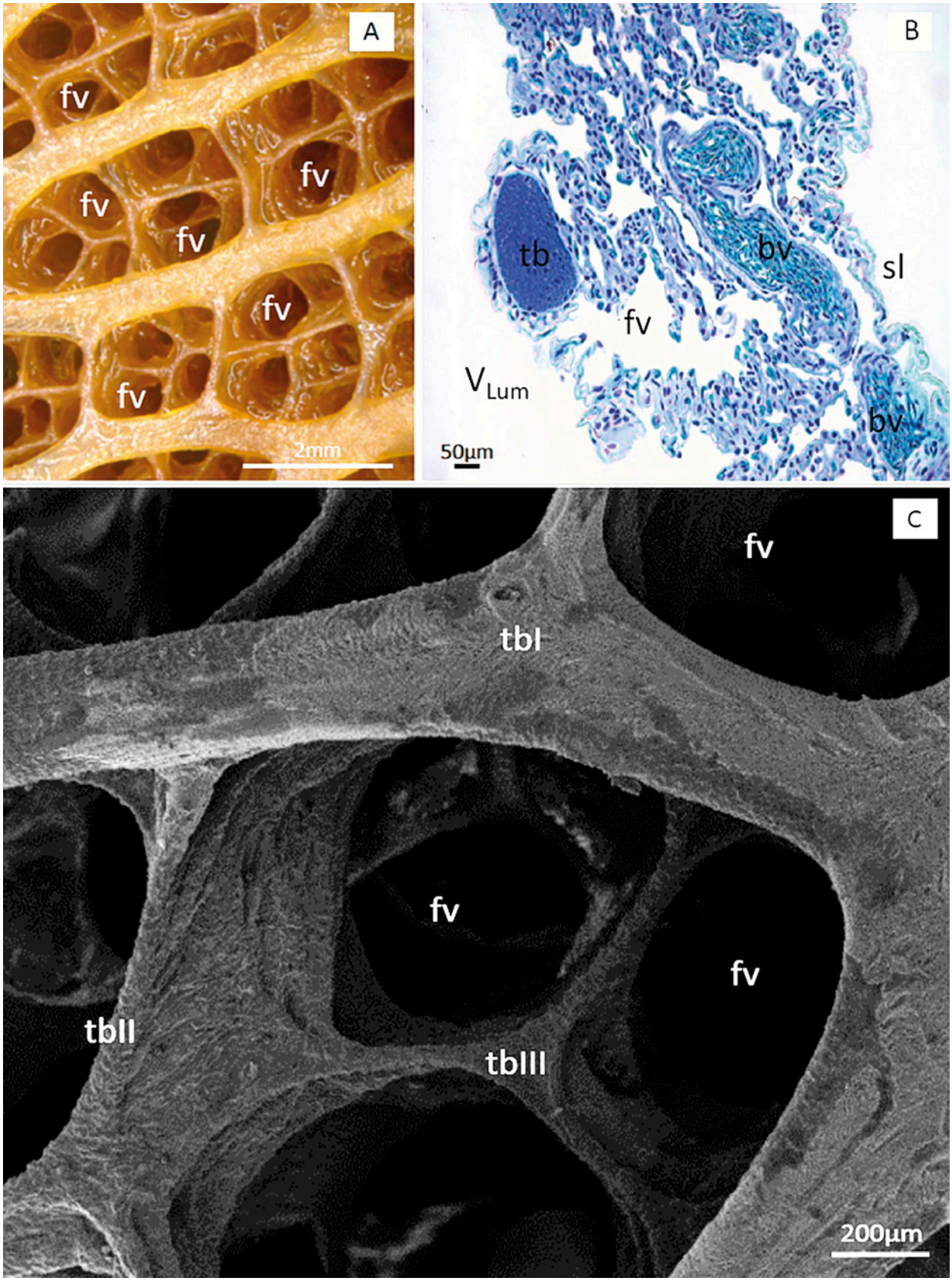

Fig. 3. Structural details of the cranial region of *Iguana iguana* lungs. (A) Stereo-micrograph (M_B=2.4 kg). (B) Histological section. Staining with toluidine blue 1% (M_B=0.026 kg). (C) Scanning electron micrograph (M_B=2.4 kg). Basal membrane (bm), blood vessel (bv), collagen fibers (cf), endoplasmic reticulum (er), endothelial cell (ec), erythrocyte (er), faveolar region (fvr), faveolus (fv), first order trabeculae (tbI), nucleus (n), pulmonary lumen (V_{Lum}), respiratory epithelium (re), second order trabeculae (tbII), serous layer (sl), third order trabeculae (tbIII), trabeculae (tb), trabecular region (tbr), type I pneumocyte (pI), type II pneumocyte (pII).

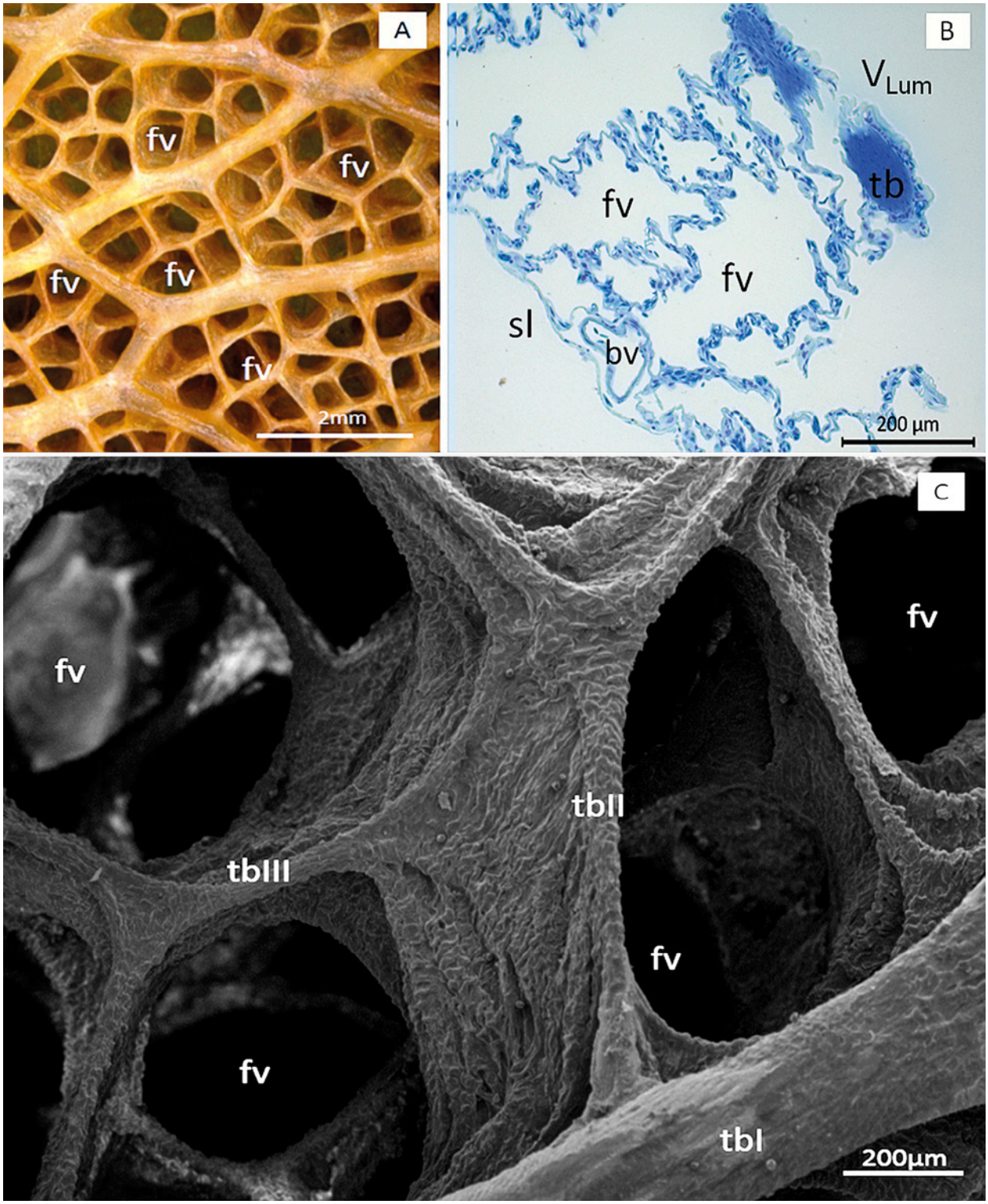

Fig. 4. Structural details of the medial region of *Iguana iguana* lungs. (A) Stereo-micrograph (M_B=2.4 kg). (B) Histological section. Staining with toluidine blue 1% (M_B=0.026 kg). (C) Scanning electron micrograph (M_B=2.4 kg). For abbreviations see Fig. 3.

posed of trabecular epithelium with a relatively large lung lumen when compared to the previous regions (Fig. 2D). The hilus could be found in the cranial region at the termination of the short intrapulmonary bronchi (Fig. 2D). A clear transitional region could be identified between medial and caudal lung regions with a significant reduction of faveolar epithelia to give way for trabecular parenchyma (Fig. 2D).

The cranial and medial regions (Figs. 3B and 4B) were composed of first, second and third order trabeculae, the latter delimiting the respiratory chambers, the faveoli (Figs. 3A and 4A). The first order trabeculae were

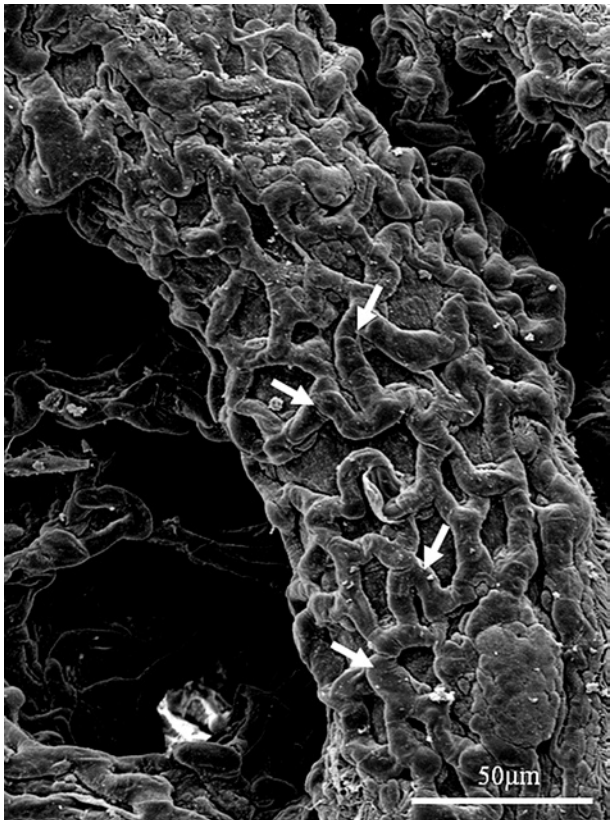

Fig. 5. Scanning electron micrograph showing the surface of trabeculae covered with capillaries (arrows) (M_B=0.546 kg).

located closest to the lumen and from the branch of these were formed second order trabeculae, which branched out forming third order trabeculae and were continuous with the interfaveolar septa (Figs. 3C and 4C). The trabeculae contained bundles of smooth muscle and were covered by blood capillaries (Fig. 5).

In the caudal region, the faveoli were absent (Figs. 6A and 6B), this region being composed of first order trabeculae fused to the pulmonary wall (Fig. 6C), featuring a trabecular parenchyma.

Pulmonary epithelium

Within the respiratory surface ciliated cells, type I and type II pneumocytes could be distinguished, the first one forming the respiratory gas exchange surface while the latter mainly secretes pulmonary surfactant. Ciliated cells were also present in parts of the surface of the first order trabeculae (Figs. 7A–D).

The epithelium lining the septa was formed by two cell types characteristic of the gas exchange regions: squamous cells located on the blood capillaries, characterized as type I pneumocytes (Fig. 8A) and cuboidal cells, containing cytoplasmic granules, located in intercapillary spaces and characterized as type II pneumocytes (Fig. 8A). Type I pneumocytes exhibited squamous appearance and consisted of a thicker region containing the nucleus, located in the central region, and a thin region formed by cytoplasmic extensions covering the surface of the capillary and forming the respiratory epithelium (Fig. 8C).

Blood capillaries could be seen on both sides of the interfaveolar septa, exposed to the lumen, forming a double capillary system. The capillaries were separated through the interfaveolar septa and only one side of each capillary was available for gas exchange (Fig. 8B). The air-blood barrier consisted of type I pneumocytes, a basement membrane, and endothelial cells forming the blood capillaries (Fig 8D).

The type II pneumocytes had a cuboid shape and were located between intercapillary spaces. Within the cytoplasm it was possible to notice numerous corpuscles inclusion present near the nucleus or in distal regions (Figs. 9A and 9B). These were formed by concentric lamellae, intensely osmiophilic and resembling lamellar bodies. At the junction regions between the type II pneumocytes it was possible to notice the presence of a junctional complex, consisting of an apical junctional zone and spot desmosomes along the lateral membrane (Fig. 9B).

Table 2. Body mass (M_B) and relative total volume of the lungs/body mass (V_L/M_B), parenchymal volume/total volume of the lungs (V_P/V_L) and parenchymal volume/body mass (V_P/M_B) of the lungs in *Iguana iguana*.

Animal	M_B (kg)	V_L/M_B ($cm^3.kg^{-1}$)	V_P/V_L ($ml.ml^{-1}$)	V_P/M_B ($cm^3.kg^{-1}$)
1	0.020	335.0	0.12	40.2
2	0.026	330.8	0.15	49.6
3	0.319	284.3	0.18	52.0
4	0.546	238.5	0.20	47.5
5	2.4	199.2	0.26	50.8
Mean	0.662	277.6	0.20	48.0
Standard deviation		58.8	0.10	4.7

Lung morphometry

The ratios between the V_L/M_B, the V_P/V_L and V_P/M_B are given in Table 2. While relative parenchymal volume (V_P/M_B) remained unchanged by increasing M_B, relative lung volume (V_L/M_B) in the specimen of 0.020 kg was equal to 335 $cm^3.kg^{-1}$ and in the specimen of 2.4 kg this value was 199.2 $cm^3.kg^{-1}$, averaging at 277.6±58.83 $cm^3.kg^{-1}$. The V_P/V_L in the lower specimen was 0.12 and in the largest specimen, this value was equal to 0.26. On average, the V_P/V_L was equal to 0.18±0.05.

The volume density of the different components of pulmonary parenchyma of *I. iguana* is presented in Table 3. The density of faveoli and interfaveolar septa

→ **Fig. 6.** Structural details of the caudal region of *Iguana iguana* lungs (A) Stereo-micrograph (M_B=2.4 kg). (B) Histological section. Staining with toluidine blue 1% (M_B=0.026 kg). (C) Electron micrograph (M_B= 2.4 kg). For abbreviations see Fig. 3.

Table 3. Volume densities (Vv) of major components of *Iguana iguana* lungs.

		Vv parenchyma			Vv interfaveolar septa		
Animal	**M_B** (kg)	**faveoli** (%)	**septa** (%)	**trabeculae** (%)	**capillaries** (%)	**type I pneumocyte** (%)	**type II pneumocyte** (%)
1	0.020	15.12	11.03	74.01	5.22	3.76	2.12
2	0.026	16.32	12.04	72.63	4.84	3.33	3.95
3	0.319	58.52	22.36	19.12	11.6	5.93	4.49
4	0.546	63.72	22.18	14.29	12.4	4.64	4.25
5	2.4	64.18	22.31	13.61	13	4.56	4.63
Mean	0.662	43.6	18.0	38.7	9.4	4.4	3.9
Standard deviation		25.5	5.9	31.6	4.0	1.0	1.0

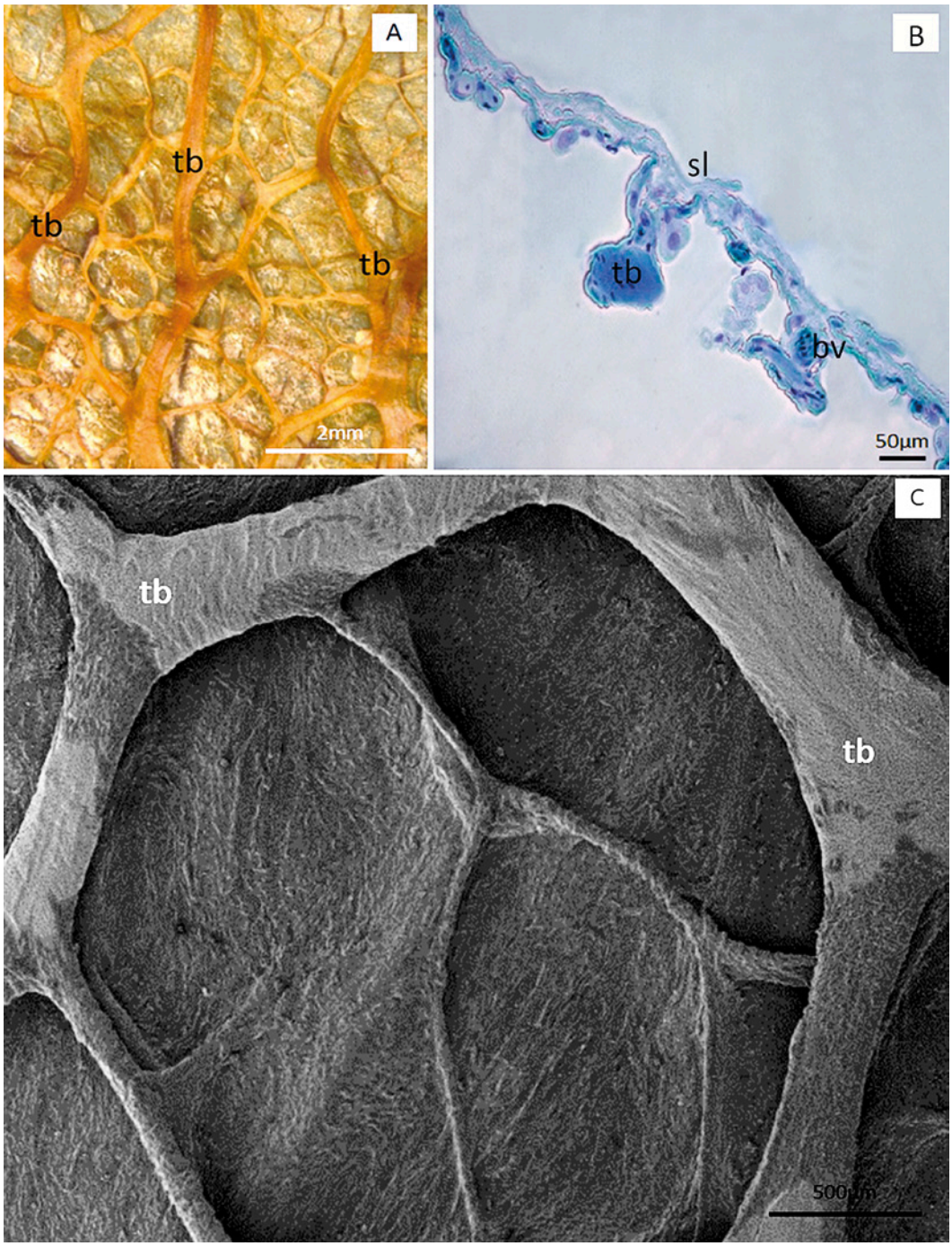

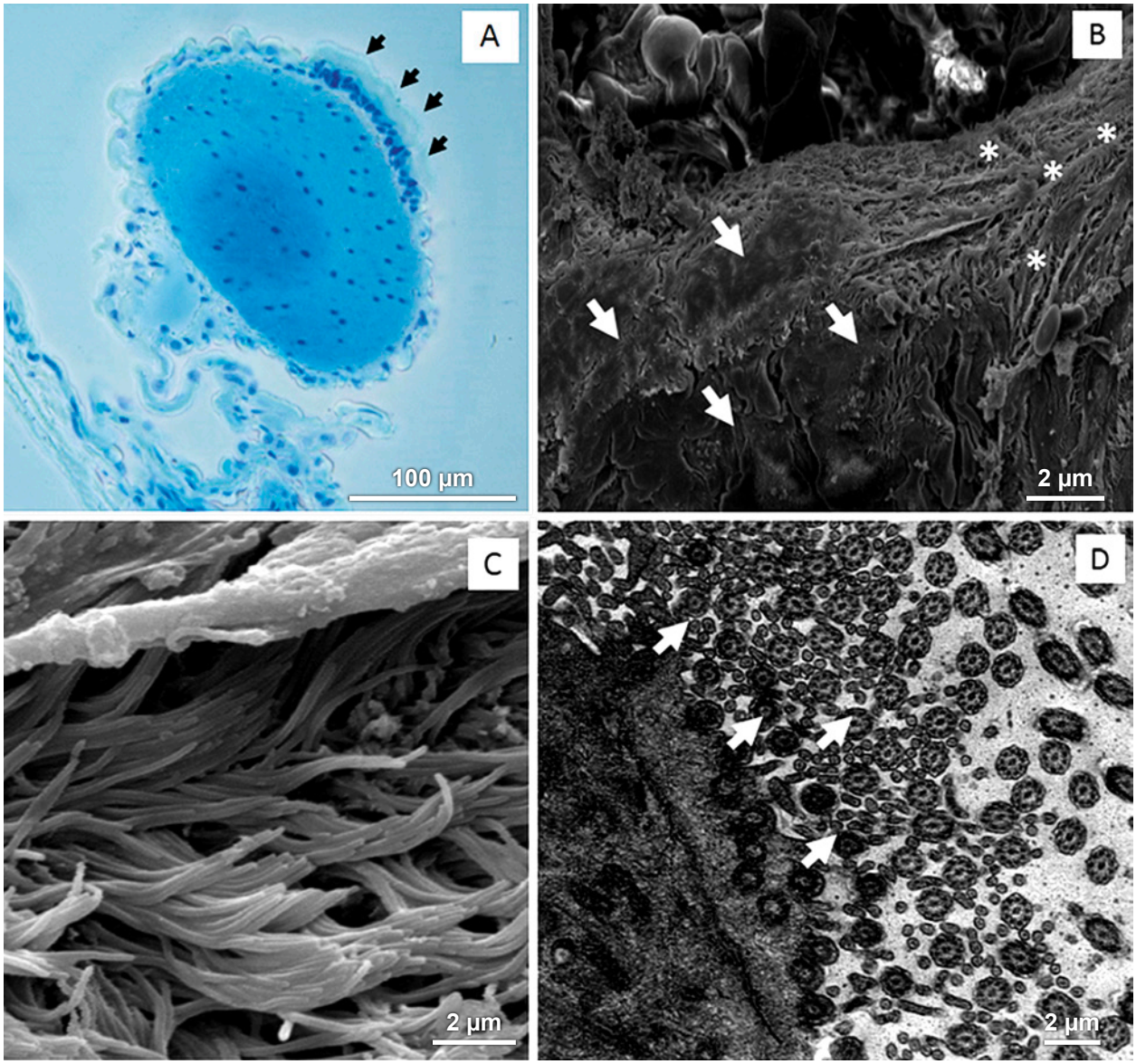

Fig. 7. (A) Histological section of the trabeculae in the lung parenchyma of *Iguana iguana* (M_B=0.319 kg), showing cilia on the surface (arrows). Staining with toluidine blue 1%. (B) Scanning electron micrograph of the trabecular surface showing the presence of non-ciliated (arrows) and ciliated regions (asterisks) (M_B=2.4 kg). (C) Scanning electron micrograph of ciliated cells (M_B=2.4 kg). (D) Transmission electron micrograph of cilia in the trabecular surface (M_B=0.319 kg).

was greater in the larger specimen, showing 64.18% and 22.31% of faveolar and septal parenchymal volume, respectively, and least in the smallest specimen, representing 15.12% and 11.03%, respectively. The inverse relationship was found for the trabecular density, which presented the greatest value (74.01%) in the smallest specimen and the lowest (13.6%) in the largest specimen. The volume densities of capillaries, type I and type II pneumocytes were greater in the largest specimen, representing 13%, 4.56% and 4.63%, respectively, and lowest in the smallest specimen, representing 5.22%, 3.76% and 2.12%, respectively. On average, 43.6±25.5% of the parenchyma corresponded to faveoli, 18.0±5.9% to septa and 38.7±31.6% to trabeculae. In the interfaveolar septa, an average of 9.4±4% (52% of the volume of the septa) corresponded to capillaries, 4.4±1% (24% of the volume of the septa) to type I pneumocytes and 3.9±1% (21% of the volume of the septa) to type II pneumocytes.

The arithmetic barrier thickness of the air-blood diffusion barrier (arithmetic mean and standard deviation) of *I. iguana* was equal to 0.58±0.10 µm (Table 4).

Discussion

The present study confirms that *Iguana iguana* possesses lungs of the transitional type, consisting of two chambers, a cranio-medial chamber composed of faveolar parenchyma, and a caudal chamber showing trabecular parenchyma, resulting in an overall heterogeneously dis-

Table 4. Comparison of the mean thickness of the diffusion barrier in *Iguana iguana* lungs (mean ± standard deviation) and other reptiles (mean, mean ± standard deviation, or range).

Species	**Mean** (μm)	Reference
Alligator mississippiensis	0.73	Meban (1980)
Anguis fragilis	0.90 ± 0.03	Meban (1980)
Calotes nemoricola	1.03 ± 0.04	Meban (1980)
Chamaeleo chamaeleon	0.73 ± 0.04	Meban (1980)
Coronella austriaca	1.02 ± 0.04	Meban (1980)
Crocodylus niloticus	1.3 (0.92 – 1.98)	Perry (1990)
Crotalus viridis oreganus	0.4 – 0.6	Luchtel and Kardong (1981)
Elaphe climacophora	0.3	Okada et al. (1962)[1]
Elaphe quadrivirgata	0.3	Okada et al. (1962)[1]
Gecko gekko	0.87 – 1.08	Perry et al. (1994)
Gekko japonicus	0.1	Okada et al. (1962)[1]
Iguana iguana	0.58 ± 0.10	This study
Lacerta muralis	0.84 ± 0.03	Meban (1980)
Lacerta viridis	0.5 – 0.7	Meban (1978)
Lacerta viridis	0.9 ± 0.03	Meban (1980)
Lacerta spp.	0.53	Cragg (1975)
Natrix natrix	1.34 ± 0.07	Meban (1980)
Pituophis melanoleucus	0.46	Stinner (1982)
Python regius	0.78 ± 0.05	Starck et al. (2012)
Rhacodactylus leachianus	0.5 – 0.6	Perry et al. (1989)
Testudo graeca	1.38 ± 0.06	Meban (1980)
Trachemys scripta	1.19 ± 0.05	Meban (1980)
Trachemys scripta	0.50	Perry (1978)
Tupinambis nigropunctatus	0.7 – 1.0	Klemm et al. (1979)
Tupinambis nigropunctatus	0.44 – 0.48	Perry (1983)
Varanus exanthematicus	0.65 ± 0.1	Perry (1983)

[1] Okada et al. (1962) report values for barrier thickness from the thinnest part of the air-blood barrier only.

tributed respiratory epithelium. This same structural type was evidenced in chamaeleonids (Klaver, 1973, 1977), agamids (Daniels *et al*., 1994) and other iguanids (Wood & Moberly, 1970; Crawford & Kampe, 1971; Bennett, 1973). In the latter group, the lungs are characterized by having two separate chambers, a short intrapulmonary bronchus and a caudal region of sac-like appearance (Perry, 1998). According to Perry (1983), although the lungs of the transitional type are formed by two separate chambers, these are considered as a single-chamber type arranged in series, due to the presence of a single communication between the chambers. Regarding the size differences found between the right and left lung in all specimens of *I. iguana*, the same was verified for other lizards. In *Diploglossus warreni*, *D. fasciatus* and *D. tenuifasciatus* (Becker, 1993), the right lung is smaller than the left, the inverse occurring in *Ophiosaurus apodus* and *O. harti* (Milani, 1894; Becker, 1993). Klein *et al*. (2005) found for the familiy Teidae a tendency for the right lung to be shorter than the left lung, but no such asymmetry in other lizard families (Cordylidae, Gerrhosauridae, Gymnophthalmidae, Lacertidae, Scincidae, and Xantusiidae). In general, there is a tendency in the partial or total reduction of the lungs in species with elongated body and reduced legs (Perry, 1998), generating larger differences between the size of the lungs.

Regarding the distribution of the parenchyma, all specimens analyzed showed a faveolar parenchyma in the cranial and medial region, with a hierarchical arrangement of first, second and third order trabeculae and trabecular parenchyma in the caudal region, consisting only of first order trabeculae. This same type of parenchymal distribution was described for teiid lizards (Klemm *et al*., 1979), geckonids (Perry *et al*., 1989, 1994), lacertids (Nielsen, 1961) and snakes (Luchtel & Kardong, 1981, Maina, 1989). Perry (1978, 1983), in studies on turtles and varanid lizards, found that more than half of the parenchyma is located in the cranial and medial regions of the lungs. Functionally, the parenchymal distribution in cranial and medial region is related to a greater specialization of these regions to carry out gas exchange, while the more sac-like caudal region does seem to provide a more ventilatory function. However, other roles have been attributed to the caudal (saccular) region of the reptilian lungs (Varde, 1951; Brattstorm, 1959; McDonald, 1959), such as gas storage or decreasing the elastic work of breathing (Perry, 1983). Intrapulmonary flow measurements undertaken recently in *I. iguana* lungs suggest the presence of a consistent pattern of airflow inside both the cranio-medial and the caudal chambers, moving air preferentially in one direction over the gas exchange epithelia (Cieri *et al*., 2014).

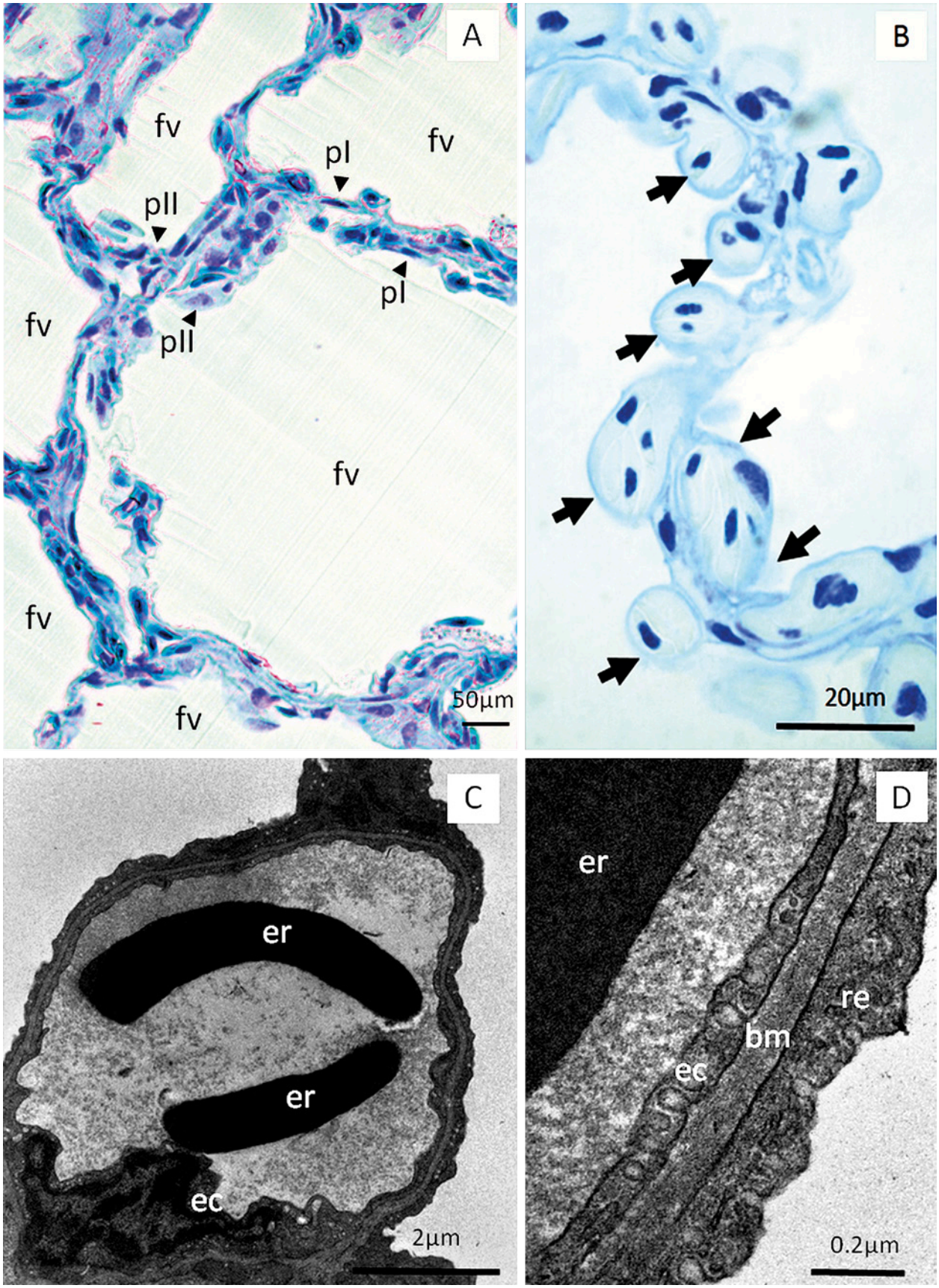

Fig. 8. Structural characterization of *Iguana iguana* lung parenchyma. (A) Histological section of the lung parenchyma in luminal view. Staining with toluidine blue 1% (M_B=0.200 kg). (B) Histological section of the interfaveolar septa indicating the presence of capillaries on both sides (arrows). Staining with toluidine blue 1% (M_B=2.4 kg). (C) Transmission electron micrograph of a type I pneumocyte showing erythrocytes and endothelial cell (M_B=0.026 kg). (D) Transmission electron micrograph of the lung air-blood barrier (M_B=0.319 kg). For abbreviations see Fig. 3.

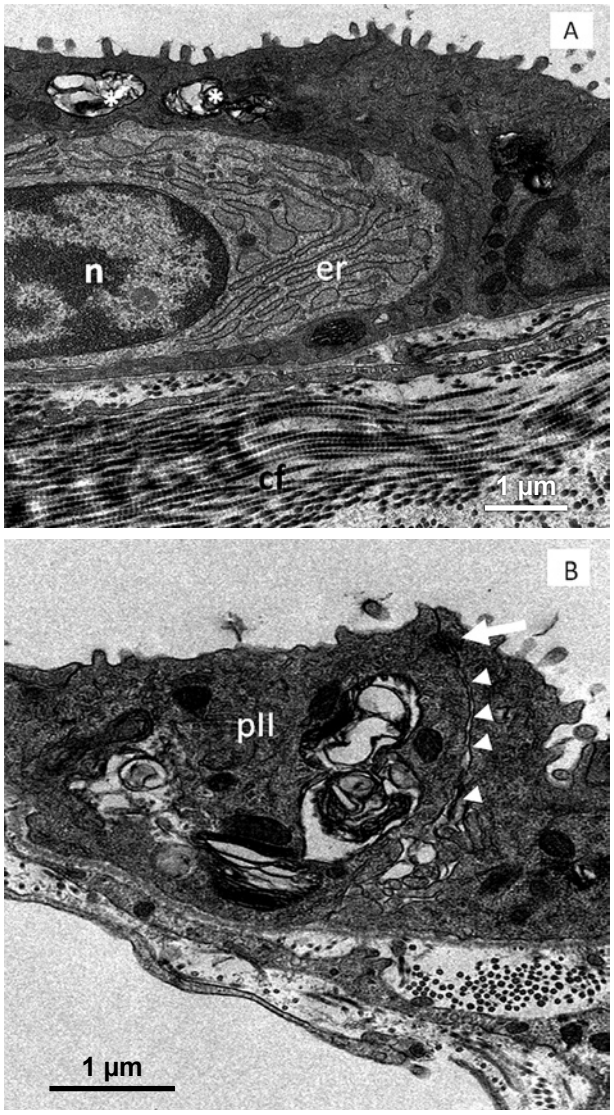

Fig. 9. Structural characterization of pneumocytes of *Iguana iguana*. (A) Transmission electron micrograph of a type II pneumocyte with lamellar bodies (*) and small microvilli-like structures, covering a cell with prominent nucleus (n) and endoplasmic reticulum (er) (M_B=0.026 kg). (B) Transmission electron micrograph showing the apical junctional zone (arrow) and spot desmosomes (arrowhead) along the lateral membrane of two neighboring type II pneumocytes (M_B=0.546 kg). For abbreviations see Fig. 3.

The muscle bundles present in trabeculae act most likely to promote the change in faveoli diameter during phases of pulmonary inflation and deflation, as suggested for other lizards and snakes (Perry & Duncker, 1978; Luchtel & Kardong, 1981). Daniels *et al*. (1994) propose a functional model to explain the role of muscle bundles in trabeculae by contraction and relaxation cycles, promoting an intrapulmonary ventilation mechanism and allowing entry and exit of air in the faveoli during ventilation.

The structure and ultrastructure of the lung epithelium of *I. iguana* did not vary with body mass and also did not differ with respect to results found in other lizards (Klemm *et al*. 1979; Meban, 1978; Perry, 1983; Perry *et al*. 1989), crocodilians (Perry, 1988) and snakes (Maina, 1989, Starck *et al*. 2012). Lung epithelium was composed of ciliated and mucous cells located on the surface of the trabeculae, type I pneumocytes located on capillaries to promote gas exchange by reducing the thickness of the air-blood barrier (Nagaishi *et al*., 1964; Maina, 2002), and type II pneumocytes located in intercapillary spaces related to the synthesis, storage and secretion of pulmonary surfactant (Daniels *et al*., 1995; Sullivan *et al*., 2001).

In *I. iguana*, surfactants may prevent atelectasis and act as an anti-adhesive compound (Daniels *et al*. 1995), preventing the adhesion of epithelial interfaveolar septa during expiration and possibly also during voluntary dives performed by this species (Moberly, 1968).

The anatomical arrangement of a double pattern of capillaries in the interfaveolar septa of *I. iguana* is found in other air breathers, such as lungfish (Maina & Maloy, 1985), amphibians (Goniakowska-Witalinska, 1978; Meban, 1977; Maina, 1989), varanid and teiid lizards (Perry, 1983), as well as embryonic stages of the mammalian lung (Klika & Anatalikova, 1978). The arrangement of blood capillaries on both sides of the septa allows only one side of the capillary to exchange gases, i.e., only half the potential surface area is available to participate in gas exchange. On the other hand, a simple capillarity pattern provides a greater surface area for gas exchange, since the whole surface of the capillary takes part in this process (Maina, 1989) being functionally more efficient than standard double capillary nets. Thus, a simple pattern of capillarity is functionally advantageous, being found in reptiles whose parenchyma is more specialized to perform gas exchange (Perry, 1983).

The nature of the diffusion barrier of the lungs of *I. iguana* showed no morphologic variations compared with those found in other reptiles and other vertebrates (Meban, 1980), consisting of type I pneumocytes, the basal membrane and capillary endothelial cells.

Regarding lung morphometrics in *I. iguana*, the total lung volume showed a strong correlation with body mass (Table 5). An increase in lung volume as a function of body mass has also been demonstrated for other iguanids (*Crotaphytus collaris* and *Sceloporus poinsettii*), teiids (*Tupinambis nigropunctatus*), varanids (*Varanus exanthematicus*), crocodilians (*Caiman sclerops*) and snakes (*Thamnophis ordinatus*, *Boa constrictor* and *Python regius*) (Tenney & Tenney, 1970; Perry, 1983; Starck *et al.*, 2012). Tenney & Tenney (1970) report V_L to show an allometric relationship with body mass as $M_B^{0.75}$ for reptiles, including in their analysis species of lizards, snakes, testudines and crocodilians. However, Alexander (1985) already suggested that determining lung volume in isolated dry-fixed lungs, as has been done by Tenney & Tenney (1970), may lead to erroneous estimates of lung volumes. Lung volume among other vertebrates has been shown to increase nearly isometrical with body mass in mammals as $M_B^{1.05}$ (Stahl, 1967), in birds as $M_B^{1.048}$ (Maina *et al*., 1989), and in amphibians as $M_B^{1.05}$ (Tenney & Tenney, 1970). Despite the fact that mammals,

Table 5. Linear OLS regressions of relationships of $\log_{10}$-lung volume (V_L) and $\log_{10}$-parenchymal volume (V_P) with $\log_{10}$-body mass (M_B) of different lizard species. N gives the number of individuals used to calculate the regression.

Species	Slope	Log_{10}–Intercept	R^2	N	Source
Lung volume					
Ameiva ameiva	0.9832±0.2455	−0.8033±0.4526	0.8004	6	W. Klein (unpublished)
Gekko gecko	0.4991±0.2745	0.3145±0.5419	0.6231	4	Perry et al. (1994)
Iguana iguana	0.8949±0.0163	−0.3271±0.0391	0.999	5	this study
Lacerta spp.	1.030±0.0358	−1.020±0.0331	0.9928	8	Cragg (1975)
'Lizards'	1.039±0.4002	−0.6107±0.8516	0.8708	3	Tenney and Tenney (1970)[a]
Salvator (*Tupinambis*) *merianae*	0.9676±0.0203	−0.670±0.0439	0.9913	22	Klein et al. (2003)
Tupinambis nigropunctatus	0.9208±0.1737	−0.8477±0.4935	0.9336	4	Perry (1983)
Parenchymal volume					
Gekko gecko	0.619±0.2636	−0.8383±0.5213	0.7287	4	Perry et al. (1994)
Iguana iguana	1.030±0.0231	−1.389±0.0554	0.9985	5	this study
Lacerta spp.	1.161±0.1129	−1.891±0.1037	0.9724	5	Cragg (1975)
Tupinambis nigropunctatus	1.123±0.2639	−2.004±0.7499	0.9005	4	Perry (1983)

[a] Among the data given by Tenney and Tenney (1970) only the lizards *Crotaphytus collaris*, *Iguana iguana* and *Scleroporus poinsettia* could be clearly associated to a given V_L and M_B.

birds, and amphibians possess significantly different lung structures and metabolic physiologies, but nonetheless show similar scaling exponents for lung volume with body mass, it seems reasonable to assume that within reptiles also an isometrical scaling relationship for lung volume with body mass could be expected. And indeed, WRIGHT & KIRSHNER (1987) report lung volume to scale as $M_B^{0.906}$ in submerged *Crocodylus porosus*, HOCHSCHEID *et al*. (2005) as $M_B^{0.9008}$ in diving marine turtles, KLEIN *et al*. (2003) found maximum lung volume in *Salvator* (*Tupinambis*) *merianae* to scale as $M_B^{0.975}$, and in the present study *I. iguana* showed lung volume to scale as $\log_{10}V_L = 0.8949.\log_{10}M_B - \log_{10}0.3271$ (Fig. 10A). Taking these discrepancies between intra- and interspecific allometric lung volume relationships among reptiles into account, we gathered data from the literature on lung volume as well as parenchymal volume of lizards with unicameral and transitional lungs and compared these data with our own results (Fig. 10). Despite only few studies having measured lung volume in lizards with sack-like lungs (Table 5) a general trend can be identified. With the exception of *Gekko gecko*, lung volume increases more isometrically with body mass, since all intraspecific slopes are close to 1.0, and the combination of all data gives an interspecific regression of $\log_{10}V_L = 1.027.\log M_B - \log_{10}0.8303$, suggesting that lung volume in lizards with unicameral and transitional lungs increases isometrically with body mass and not as predicted by TENNEY & TENNEY (1970) as $M_B^{0.75}$. The regression obtained for *Gecko gecko*, may indicate a different scaling relationship in this species, but too few data are available and the regression also shows a very poor fit, needing data over a wider range of body masses to verify the results.

Parenchymal lung volume also increases isometrically with body mass in *I. iguana*, *Lacerta* spp. and *Tupinambis nigropunctatus* (Table 5, Fig. 10B), but not in *Gekko gecko*, in the latter species probably due to the reasons mentioned before. Interestingly, combing the data for the three species with unicameral lungs (*Lacerta* spp., *T. nigropunctatus*, and *G. gecko* results in a linear regression with its slope not being significantly different from the regression of the transitional type *I. iguana* lung, but the intercepts are significantly different ($\log_{10}V_P = 1.083.\log M_B - \log_{10}1.835$ *versus* $\log_{10}V_P = 1.030.\log M_B - \log_{10}1.389$), just as could be expected from the general morphology of these lungs, where respiratory epithelia in unicameral lungs are exclusively located on the inner wall of the lung chambers, but in transitional lungs few septa dissect the central lung lumen (PERRY, 1998).

The present study suggests that lung volume and parenchymal volume increase in a greater proportion than the metabolic rate of *I. iguana*, which showed an allometric exponent value equal to 0.73 (MAXWELL *et al*., 2003). The body mass standardized V_L showed an inverse relationship, being greater in the smaller animals when compared to the largest iguana. Similar results were observed in *Gekko gecko* and *Crocodylus niloticus* (PERRY, 1994, 1988), indicating that animals of lower body mass possess greater lung volumes per unit body mass. The strong correlation found between parenchymal volume and body mass in *I. iguana*, increasing parenchymal density with increasing body size, was caused by a greater internal compartmentalization of the lungs, as indicated by the increasing densities of the faveoli and the interfaveolar septa (Table 3).

The volume density of trabeculae indicates a reduction throughout the body mass increase (Table 3). However, it was observed that the smaller specimens (0.020 and 0.026 kg, respectively) showed a lower density in interfaveolar septa, and may have contributed to the greater values of trabecular density found when compared to animals with larger body mass. The trabeculae were composed of 70% smooth muscle and 18.2% capillaries. The percentages of smooth muscle and capillaries are 75.9%

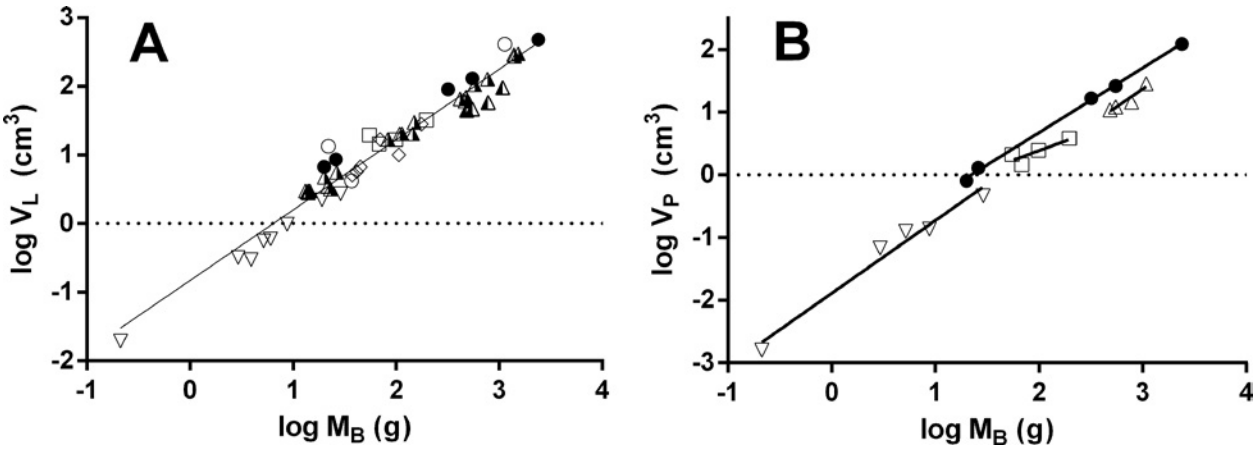

Fig. 10. Log-transformed values of (A) lung volume (V_L) as function of body mass (M_B) obtained in the present study (*Iguana iguana*; ●), or extracted from Cragg (1975) (*Lacerta* spp.; ▽), Klein et al. (2003) (*Salvator* (*Tupinambis*) *merianae*; ◭), W. Klein (unpublished) (*Ameiva ameiva*; ◇), Perry (1983) (*Tupinambis nigropunctatus*; ◭), Perry et al. (1994) (*Gekko gecko*; □), and Tenney and Tenney (1970) (*Crotaphytus collaris*, *Iguana iguana*, *Scleroporus poinsettia*; ○). The line represents the linear regression of all data points combined, given by the formula: $\log_{10}V_L = 1.027.\log_{10}M_B - 0.8303$. Log-transformed values of (B) parenchymal volume (V_P) in function of body mass (M_B) obtained in the present study (*Iguana iguana*; ●), or extracted from Cragg (1975) (*Lacerta viridis*; ▽), Perry (1983) (*Tupinambis nigropunctatus*; △), and Perry et al. (1994) (*Gekko gecko*; □). The intraspecific regressions are given in Table 5.

and 5.1% in *Tupinambis nigropunctatus*, respectively, and in *Varanus exanthematicus* on average 54% and 16%, respectively (Perry, 1983).

The higher bulk density of capillaries, type I and type II pneumocytes in specimens of greater body mass is related to the greater amount of parenchyma, since these components are within interfaveolar septa and the volume density of septa is shown ascending from smaller individuals (0.020 kg to 0.026 kg) to the largest ones (0.319 kg, 0.546 kg and 2.4 kg) (Table 3). This is the first study to determine the volume density of type I and type II pneumocytes within respiratory epithelia of reptiles. On average, the capillaries accounted for 52% of the total volume of septa. Similar values (70%) were found for *Gekko gecko*, a species with unicameral lungs and double standard capillarity (Perry, 1994). Since the thickness of the blood-air diffusion barrier in *I. iguana* and other reptiles was found to be similar (Table 4), it is reasonable to assume the occurrence of structural conservation of the pulmonary epithelium allowing gas exchange. Thus, in *I. iguana*, like in other reptiles, the diffusion barrier seems to be as thin as possible without prejudice to its mechanical stability, and in order to favor gas exchange. However, in a recent study Gillooly *et al*. (2016) found no correlation between barrier thickness and body mass in ectothermic vertebrates.

I. iguana, as well as other vertebrates, meet their metabolic demands for locomotion mainly through aerobic metabolism (Moberly, 1968), which comprises a series of coordinated steps constituting the oxygen cascade (Farmer & Hicks, 2000). According to these authors, restrictions on certain points of the cascade can significantly affect gas exchange. Wang *et al*. (1997) found a decrease in pulmonary ventilation and oxygen extraction in *I. iguana* with the progressive increase in locomotor activity, attributing this to a mechanical constraint caused by the simultaneous occurrence of costal ventilation and mobility (Carrier, 1987). The lateral undulations of the body reduce the effectiveness of the costal breathing movements because the intercostal muscles are also used in body movement during locomotion, contracting alternately and not simultaneously, as required during ventilation. Farmer & Hicks (2000) found that both ventilatory air flow and pulmonary blood flow are affected in *I. iguana* by increasing locomotor activity. Ventilation is reduced due to muscular restrictions and blood flow due to pressure increases in the trunk, causing constriction of blood vessels. Thus, *I. iguana* is unable to expand its locomotor activity associated with adequate ventilation (Frappell *et al.*, 2002).

With increasing body mass there is a reduction in lung volume per unit of body mass, whereas the parenchymal volume remains constant. This indicates that neonate and juvenile animals have relatively larger lungs per unit body mass than adults, although they show the same proportion of parenchyma, potentiating a greater metabolic rate. These inferences are supported by activity pattern found in this species. Swanson (1950) and Henderson (1974) found that juvenile *I. iguana* are seen predominantly foraging on the ground and have greater metabolic rates than adults (Troyer, 1984) and, thus could possess a greater metabolic scope when compared to adults.

Conclusions

In conclusion, *I. iguana* possess lungs that bring together characteristics considered simple for gas exchange, but are functionally well adapted to the metabolic demands of the species. The functional morphology of the lungs

in *I. iguana* seems to play an important role to meet the metabolic demands, influencing the lifestyle dependent on different body masses. The simple pulmonary structure and potential restrictions between the joint occurrence of locomotion and respiration can be decisive in the adoption of high or low activity pattern, associated with different body masses and their respective niches. Our data, as well as other literature data, suggest that lung volume scales proportionally to body mass, and thereby significantly different from the pattern described previously for reptiles, recommending further analysis of scaling relationships of respiratory system variables among reptiles.

Acknowledgements

The authors gratefully acknowledge the Electron Microscopy Laboratory at the Oswaldo Cruz Foundation (CpqGM-Fiocruz-Salvador-BA) for enabling the transmission and scanning electron microscopy analysis. ALC, WK and ASA were research members of the National Institute of Science and Technology in Comparative Physiology (INCT em Fisiologia Comparada; Fundação de Amparo à Pesquisa do Estado de São Paulo (FAPESP) 2008/57712-4, Conselho Nacional de Desenvolvimento Tecnológico e Científico (CNPq) 573921/2008-3). DP thanks the Foundation for Supporting Research in the State of Bahia (FAPESB) for awarding scholarships.

Disclosure Statement: the authors declare no competing financial interests.

References

Allegra, L., Bossi, R. & Braga, P. (1985): Influence of surfactant on mucociliary transport. – European Journal of Respiratory Disease, Suppl., **142**: 71–76.

Alexander, R.M. (1985): Mechanics of posture and gait of some large dinosaurs. – Zoological Journal of Linnean Society, **83**: 1–25.

Andrews, R.M. & Pough, F.H. (1985): Metabolism of squamate reptiles: Allometric and ecological relationships. – Physiological Zoology, **58**: 214–231.

Brattstrom, B.H. (1959): The functions of the air sac in snakes. – Herpetologica, **15**: 103–104.

Becker, H.O. (1993): Vergleichende Untersuchungen am respiratorischen Apparat anguimorpher Eidechsen: Eine stammesgeschichtliche Deutung. Dissertation, Rheinische Friedrich-Wilhelms-Universitat Bonn, Germany.

Bennett, A.F. (1973): Blood physiology and oxygen transport during activity in two lizards, *Varanus gouldii* and *Sauromalus hispidus*. – Comparative Biochemistry and Physiology A, **46**: 673–690.

Bennett, A.F. & Dawson, W.R. (1976): Metabolism. In: Gans, C., Dawson, W.R. (Eds.). Biology of the Reptilia, Vol. 5. London: Academic Press, pp. 127–223.

Beuchat, C.A. & Vleck, D. (1990): Metabolic consequences of viviparity in a lizard, *Sceloporus jarrovI*. – Physiological Zoology, **63**: 555–570.

Carrier, D.R. (1987): The evolution of locomotor stamina in tetrapods: circumventing a mechanical constraint. – Paleobiology, **13**: 326–341.

Cieri, R.L., Craven, B.A., Schachner, E.R. & Farmer, C.G. (2014): New insight into the evolution of the vertebrate respiratory system and the discovery of unidirectional airflow in iguana lungs. – PNAS, **111**: 17218–17223.

Cragg, P. (1975): Respiration and body weight in the reptilian genus *Lacerta*: A physiological, anatomical and morphometric study. PhD thesis. University of Bristol, UK.

Crawford, E.C. & Kampe, G. (1971): Physiological responses of the lizard *Sauromalus obesus* to changes in ambient temperature. – American Journal of Physiology, **220**: 1256–1260.

Cruz-Orive L.M. & Weibel, E.R. (1990): Recent stereological methods for cell biology: a brief survey. – American Journal of Physiology, **258**: L148–156.

Daniels, C.B., McGregor, L.K., Nicholas, T.E. (1994): The Dragon's breath: A model for the dynamics of breathing and faveolar ventilation in agamid lizards. – Herpetologica, **50**: 251–261.

Daniels, C.B., Orgeig, S. & Smits, A.W. (1995): The composition and function of reptilian pulmonary surfactant. – Respiration Physiology, **102**: 121–135.

Dawson, W.R. & Bartholomew, G.A. (1956): Relation of oxygen consumption to body weight, temperature, and temperature acclimation in lizards *Uta stansburiana* and *Sceloporus occidentalis*. – Physiological Zoology, **29**: 40–51.

Duncker, H.R. (1978): General morphological principles of amniotic lungs. In: Piiper, J. (Ed.). Respiratory Function in Birds, Adult and Embryonic. – Proceedings in Life Sciences, pp. 2–15.

Farmer, C.G. & Hicks, J.W. (2000): Circulatory impairment induced by exercise in the lizard *Iguana iguana*. – Journal of Experimental Biology, **203**: 2691–2697.

Frappell, P., Schultz, T. & Christian, K. (2002): Oxygen transfer during aerobic exercise in a varanid lizard *Varanus mertensi* is limited by circulation. – Journal of Experimental Biology, **205**: 2725–2736.

Gillooly, J.F., Gomez, J.P., Mavrodiev, E.V., Rong, Y. & McLamore, E.S. (2016): Body mass scaling of passive oxygen diffusion in endotherms and ectotherms. – PNAS, **113**: 5340–5345.

Goniakowska-Witalinska, L. (1978): Ultrastructure and morphometric study of the lung of the European salamander, *Salamandra salamandra* L. – Cell Tissue and Research, **191**: 343–356.

Henderson, R.W. (1974): Aspects of the ecology of the juvenile common iguana (*Iguana iguana*). – Herpetologica, **30**: 327–332.

Hochscheid, S., McMahon, C.R., Bradshaw, C.J.A., Maffucci, F., Bentivegna, F. & Hays, G.C. (2007): Allometric scaling of lung volume and its consequences for marine turtle diving performance. – Comparative Biochemistry and Physiology A, **148**: 360–367.

Howard, C.V. & Reed, M.G. (2005): Unbiased stereology: three-dimensional measurement in microscopy. Second edition. Oxon, New York: Garland Science/BIOS Scientific Publishers.

Hughes, G.M. (1977): A morphological and ultrastructural comparison of some vertebrate lungs. In: Klike, E. (Ed.). XIX Con-

gressus Morphologicus Symposia. Charles University, Prague, pp. 393–405.

Karasov, W.H. & Anderson, R.A. (1998): Correlates of average daily metabolism of field-active zebra-tailed lizards (*Callisaurus draconoides*). – Physiological Zoology, **71**: 93–105.

Klaver, C.J.J. (1973): Lung-anatomy: aid in Chameleon-taxonomy. – Beaufortia, **20**: 155–177.

Klaver, C.J.J. (1977): Comparative lung-morphology in the genus *Chamaeleo* Laurenti, 1768 (Sauria: Chamaeleonidae) with a discussion of taxonomic and zoogeographic implications. – Beaufortia, **25**: 167–199.

Klaver, C.J.J. (1979): A review of *Brookesia* systematics with special reference to lung-morphology (Reptilia: Sauria: Chamaeleonidae). – Bonner Zoologische Beiträge, **30**: 162–175.

Klein, W., Abe, A.S. & Perry, S.F. (2003): Static lung compliance and body pressures in *Tupinambis merianae* with and without post-hepatic septum. – Respiration Physiology and Neurobiology, **135**: 73–86.

Klein, W., Reuter, C., Böhme, W. & Perry, S.F. (2005): Lungs and mesopneumonia of scincomorph lizards (Reptilia: Squamata). – Organisms Diversity and Evolution, **5**: 47–57.

Klemm, R.D., Gatz, R.N., Westfall, J.A. & Fedde, M.R. (1979): Microanatomy of the lung parenchyma of a tegu lizard *Tupinambis nigropunctatus*. – Journal of Morphology, **161**: 257–279.

Klika, E. & Anatalikova, L. (1978): Prenatal development of human lung. In: Klika, E. (Ed.). XIX Congressus Morphologicus Symposia. Charles University, Prague, pp. 385–391.

Luchtel, D.L. & Kardong, K.V. (1981): Ultrastructure of the lung of the rattlesnake, *Crotalus viridis oreganus*. – Journal of Morphology, **169**: 29–47.

Maina, J.N. (1989): The morphology of the lung of the black mamba *Dendroaspis polylepis* (Reptilia: Ophidia: Elapidae). A scanning and transmission electron microscopic study. – Journal of Anatomy, **167**: 31–46.

Maina, J.N. (2002): Structure, function and evolution of the gas exchangers: comparative perspectives. – Journal of Anatomy, **201**: 281–304.

Maina, J.N., King, A.S. & Settle, G. (1989): An allometric study of pulmonary morphometric parameters in birds, with mammalian comparisons. – Philosophical Transactions of the Royal Society of London B. Biological Sciences, **326**: 1–57.

Maina, J.N. & Maloy, G.M. (1985): The morphometry of the lung of the African lungfish (*Protopterus aethiopicus*): its structural-functional correlations. – Proceedings of Royal Society, **224**: 399–420.

Maina, J.N., Maloy, G.M., Warui, C.N., Njogu, E.K. & Kokwaro, E.D. (1989): Scanning electron microscope study of the morphology of the reptilian lung: the Savanna monitor lizard *Varanus exanthematicus* and the pancake tortoise *Malacochersus tornieri*. – The Anatomical Record, **224**: 514–522.

Maxwell, L., Jacobson, E. & McNab, B. (2003): Intraspecific allometry of standard metabolic rate in green iguanas, *Iguana iguana*. – Comparative Biochemistry and Physiology A, **136**: 301–310.

McDonald, H.S. (1959): Respiratory functions of the ophidian air sac. – Herpetologica, **15**: 193–198.

McNab, B. (2002): The Physiological Ecology of Vertebrates: a View from Energetics. Cornell University Press, Ithaca.

Meban, C. (1977): Ultrastructure of the respiratory epithelium in the lungs of the tortoise, *Testudo graeca*. – Cell Tissue and Research, **181**: 167–275.

Meban, C. (1978): Functional anatomy of the lungs of the green lizard, *Lacerta viridis*. – Journal of Anatomy, **125**: 421–431.

Meban, C. (1980): Thickness of the air-blood barriers in vertebrate lungs. – Journal of Anatomy, **131**: 299–307.

Milani, A. (1894): Beitrage zur Kenntnis der Reptilienlunge. I. Lacertilia. – Zoologische Jahrbücher. Abteilung für Anatomie und Ontogenie der Tiere, **7**: 545–592.

Moberly, W.R. (1968): The metabolic responses of the common iguana, *Iguana iguana*, to walking and diving. – Comparative Biochemistry and Physiology, **27**: 21–32.

Nagaishi, C., Okada, Y., Ishiko, S. & Daido, S. (1964): Electron microscopic observations of the pulmonary alveolI. – Experimental Medicine and Surgery, **22**: 81–117.

Nielsen, B. (1961): On the regulation of respiration in reptiles. I. The effect of temperature and CO_2 on the respiration of lizards (*Lacerta*). – Journal of Experimental Biology, **38**: 301–314.

Okada, Y., Ishiko, S., Daido, S., Kim, J., Ikeda, S. (1962): Comparative morphology of the lung with special reference to the alveolar lining cells. II. Lung of the Reptilia. – Acta Tuberculosea Japonica, **12**: 1–10.

Perry, S.F. (1978): Quantitative anatomy of the lungs of the red-eared turtle, *Pseudemys scripta elegans*. – Respiration Physiology, **35**: 245–262.

Perry, S.F. (1983): Reptilian lungs: functional anatomy and evolution. – Advances in Anatomy, Embryology and Cell Biology, **79**. 1–81.

Perry, S.F. (1988): Functional morphology of the lungs of the Nile crocodile, *Crocodylus niloticus*: non-respiratory parameters. – Journal of Experimental Biology, **117**: 99–117.

Perry, S.F. (1990): Gas exchange strategy in the Nile crocodile: a morphometric study. – Journal of Comparative Physiology B, **159**: 761–769.

Perry, S.F. (1998): Lungs: comparative anatomy, functional morphology, and evolution. In: Gans, C. (Ed.). Biology of the Reptilia, Vol. 19. Ithaca: Society for the Study of Amphibians and Reptiles, pp. 1–92.

Perry, S.F. & Duncker, H.R. (1978): Lung architecture, volume and static mechanics in five species of lizards. – Respiration Physiology, **34**: 61–81.

Perry, S.F., Bauer, A.M., Russell, A.P., Alston, J.T. & Maloney, J.E. (1989): Lungs of the gecko *Rhacodactylus leachianus* (Reptilia: Gekkonidae): a correlative gross anatomical and light and electron microscopic study. – Journal of Morphology, **199**: 23–40.

Perry, S.F., Hein, J. & Vandieken, E. (1994): Gas-exchange morphometry of the lungs of the Tokay, *Gekko gecko* L (Reptilia, Squamata, Gekkonidae). – Journal of Comparative Physiology B, **164**: 206–214.

Powell, F.L. & Hokins, S.R. (2004): Comparative physiology of lung complexity: implications for gas exchange. – News in Physiological Sciences, **19**: 55–60.

Stahl, W.R. (1967): Scaling of respiratory variables in mammals. – Journal of Applied Physiology, **22**: 453–460.

Starck, J.M., Aupperle, H., Kiefer, I., Weimer, I., Krautwald-Junghanns, M. & Pees, M. (2012): Morphological respiratory diffusion capacity of the lungs of ball pythons (*Python regius*). – Zoology, **115**: 245–254.

STINNER, J.N. (1982): Functional anatomy of the lung of the snake *Pituophis melanoleucus*. – American Journal of Physiology-Regulatory, Integrative and Comparative Physiology, **243**: 251–257.

SULLIVAN, L.C., ORGEIG, S., WOOD, P.G. & DANIELS, C.B. (2001): The ontogeny of pulmonary surfactant secretion in the embryonic green sea turtle (*Chelonia mydas*). – Physiological and Biochemical Zoology, **74**: 493–501.

SWANSON, P.L. (1950): The iguana *Iguana iguana iguana* (L.). – Herpetologica, **6**: 187–193.

TENNEY, S.M. & TENNEY, J.B. (1970): Quantitative morphology of cold-blooded lungs: amphibia and reptilia. – Respiration Physiology, **9**: 197–215.

TROYER, K. (1984): Diet selection and digestion in *Iguana iguana*: the importance of age and nutrient requirements. – Oecologia, **61**: 201–207.

VARDE, M. (1951): The morphology and histology of the lung in snakes. – Journal of the University of Bombay, **19**: 79–89.

VAN MARKEN-LICHTENBELT, W., WESSELING, H.R., VOGEL, J. & ALBERS, K.B.M. (1993): Energy budgets in free-living green iguanas in a seasonal environment. – Ecology, **74**: 1157–1172.

VERNET, R., CASTANET, J. & BAEZ, M. (1995): Comparative water flux and daily energy expenditure of lizards of the genus *Gallotia* (Lacertidae) from the Canary Islands. – Amphibia-Reptilia, **16**: 55–66.

WANG, T., CARRIER, D. & HICKS, J. (1997): Ventilation and gas exchange in lizards during treadmill exercise. – Journal of Experimental Biology, **200**: 2629–2639.

WRIGHT, J. & KIRSHNER, D. (1987): Allometry of lung volume during voluntary submergence in the saltwater crocodile *Crocodylus porosus*. – Journal of Experimental Biology, **130**: 433–436.

WOLF, S. (1933): Zur Kenntnis von Bau und Funktion der Reptilienlungen. – Zoologische Jahrbücher. Abteilung für Anatomie und Ontogenie der Tiere, **57**: 139–190.

WOOD, S. & MOBERLY, W. (1970): The influence of temperature on the respiratory properties of iguana blood. – Respiration Physiology, **10**: 20–29.

WOOD, S., JOHANSEN, K., GLASS, M.L. & MALOY, G. (1978): Aerobic metabolism of the lizard *Varanus exanthematicus*: effects of activity, temperature, and size. – Journal of Comparative Physiology B, **127**: 331–336.